# Coalescence of atomically precise clusters on graphenic surfaces

*Atanu Ghosh[1], Thalappil Pradeep[1] and J. Chakrabarti[2]*

*[1]DST Unit of Nanoscience (DST UNS) and Thematic Unit of Excellence (TUE), Department of Chemistry, Indian Institute of Technology Madras, Chennai 600 036, India*

*E-mail: pradeep@iitm.ac.in*

*[2]S. N. Bose National Centre for Basic Sciences, Block-JD, Sector-III, Salt Lake, Kolkata 700091, India*

---

We show that an atomically precise and monolayer protected cluster, $Au_{25}(SCH_2CH_2Ph)_{18}$ ($SCH_2CH_2Ph$-phenylethane thiolate ligand), when mixed with chemically synthesized graphene, undergoes coalescence to yield monodisperse clusters, assigned to ~ $Au_{135}(SCH_2CH_2Ph)_{57}$. This conversion depends on the amount of the parent cluster and graphene in the reaction mixture. Graphene surface at the end of the reaction shows larger clusters attached on it. The conversion rate indicates sluggish dynamics while the coarsening takes place. The chemical transformation occurs at deformable surfaces at reduced particle densities and the observations are supported by a simple theoretical model.

---

Diffusion and migration of metal atoms on graphite surfaces are well studied theoretically and experimentally over the past two decades.[1-4] Very recently, graphene-metal and graphene-metal nanoparticle composites have become hot topics of research because of their biological,[5] magnetic,[6] electrochemical,[7] optical[8] and environmental[9] properties. Heiz, Landman and colleagues have shown the mobility of naked palladium clusters on graphene surfaces.[10] Such clusters are, however, stable only in vacuum as they are unprotected. In the present work, we show that stable and atomically precise clusters of noble metals undergo rapid transformation to their larger analogues at graphenic interfaces. Atomically precise analogues of noble metals, protected with monolayers, referred to as quantum clusters (QCs), nanomolecules, clusters or super atoms are stable materials which can be prepared by solution chemistry. Among the most studied clusters in this class are $Au_{25}$, $Au_{36}$, $Au_{38}$ and $Au_{102}$ (with specific number of ligands, see below) for which crystal structures are known.[11-15] These electronically stable clusters and their structurally stable analogs, $Au_{13}$, $Au_{55}$ and $Au_{144}$ are also studied for some time.[16-18] Clusters can undergo inter-conversion from one form to the other under suitable conditions.[19] For instance, larger clusters etch to smaller ones in the presence of excess ligands.[20] Inter-conversion becomes feasible especially at liquid-liquid interfaces which create active environment for such reactions.[21] Interfaces can present active surfaces which could lead to systematic coalescence of clusters. In this context, it is important to recall that gold clusters undergo anomalous diffusion at the basal plane of graphite, termed as Lévy flights.[1] In this work, we use the large and atomically thin surface of

graphene for the coalescence of $Au_{25}(SCH_2CH_2Ph)_{18}$ to $Au_{135}(SCH_2CH_2Ph)_{57}$, where $SCH_2CH_2Ph$ is a ligand protecting the cluster core of finite number of gold atoms. We will refer to these molecules as $Au_{25}$ and $Au_{135}$ in the subsequent discussion. We observe that the conversion takes place on the graphene surface and it depends on both graphene and $Au_{25}$ concentrations. Our results point to the active role of interfaces in facilitating the conversion. We theoretically model the role of the surface in stabilizing the large clusters. Formation of specific clusters of precise composition on active surfaces may be important to create novel catalysts.

We have prepared the parent material $Au_{25}$, by our in-house-developed method. The concept of slow reduction was used to prepare this material.[22] To $HAuCl_4$ in a methanol:tetrahydrofuran (THF) mixture (100 mg, 25 mM), 3 equivalents of phenylethanethiol (PET) was added under stirring at room temperature. After 30 minutes, 10 equivalents of ice cold solution of $NaBH_3CN$ in 2 mL cold water was added and the solution was kept stirring at room temperature. Formation of $Au_{25}$ took 42 hours. The evolution of $Au_{25}$ was investigated by UV-vis spectroscopy and matrix assisted laser desorption ionization mass spectrometry (MALDI MS) as a function of time using DCTB (trans-2-[3-(4-tert-butylphenyl)-2-methyl-2-propenylidene] malononitrile) as the matrix. The prepared $Au_{25}$ shows well defined optical features[23] with a characteristic mass peak at m/z 7391 in the positive ion spectrum (with a $\Delta$m of 15), in agreement with the theoretical mass of 7391 for $Au_{25}(SCH_2CH_2Ph)_{18}^+$ and a fragmentation product at m/z 6055 (marked in Fig. 1 by *)[23] due to $Au_{21}(SCH_2CH_2Ph)_{14}^+$. About 100 µL of as-synthesized $Au_{25}$ in THF was added to a 3 mL suspension of chemically synthesized graphene[24-25] (0.01 wt %) in water which was thoroughly cleaned and contained no impurities. Rapid disappearance of the color of the mixture was noticed and almost simultaneously a black matter suspended at the top. The solution became colorless. The black suspended matter was characterized with MALDI MS study using DCTB as the matrix. MALDI MS of this material as a function of reaction time is shown in Fig. 1. This transformation shows a gradual evolution of a peak

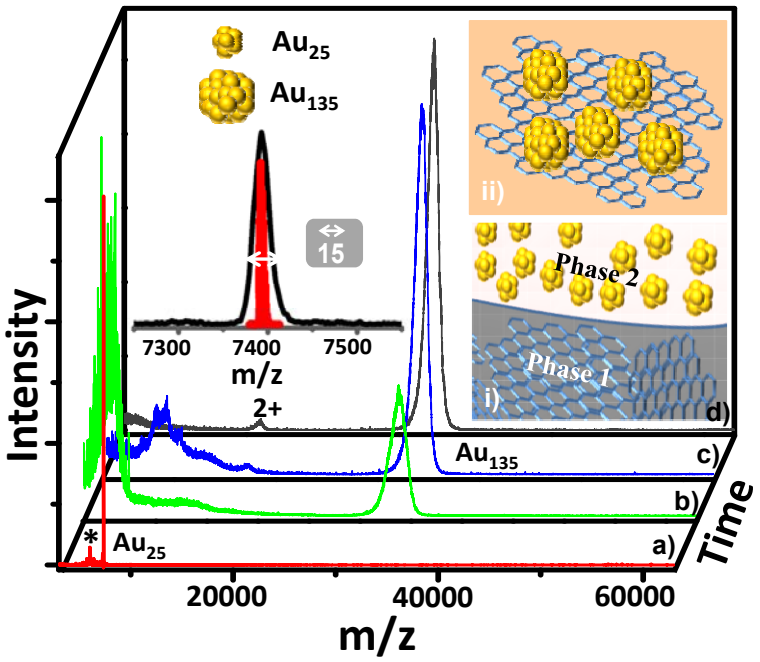

**Fig. 1.** (a-d) Time dependent positive ion MALDI MS study of the conversion of $Au_{25}$. At zero time (a) shows a peak corresponding to pure $Au_{25}$ (main peak at m/z 7391 and a fragment at m/z 6055). The fragment is shown with a star (*). The main peak is expanded on the left. After certain time, mixtures of clusters including $Au_{135}$ were formed (b). With increasing time, the peak of $Au_{135}$ increases and peaks corresponding to lower m/z decrease in intensity (c). (d) Spectrum showing that $Au_{135}$ has been formed after a certain time for a particular concentration of graphene and $Au_{25}$. Dication (2+) of $Au_{135}$ is seen in MALDI MS, marked on trace (d). Insets show i) the presence of two phases of the reaction mixture, cluster ($Au_{25}$) and graphene and ii) the final product of $Au_{135}$ on the graphene surface.

at m/z 34.4 kDa assigned to $Au_{135}(SCH_2CH_2Ph)_{57}^+$ along with the simultaneous disappearance of the peak due to $Au_{25}(SCH_2CH_2Ph)_{18}^+$. The assignment may have a slight uncertainty as other Au/$SCH_2CH_2Ph$ combinations are possible. Confirmation of the assignment comes from the appearance of the di-cation, $[Au_{135}(SCH_2CH_2Ph)_{57}]^{2+}$ at m/z 17.2 kDa. Occurrence of dication is a standard feature seen in MALDI MS of such large clusters.[26] This complete conversion occurs at a finite time interval after which no $Au_{25}$ was detected in the solution, at the interface. In between these two times, several features were observed in the lower mass region (m/z 8000 to 18000) which are attributed to intermediate products. From our time dependent study, we have shown that $Au_{33}$, $Au_{38}$, $Au_{55}$ and some other clusters (the ligand shell is neglected in this description) were formed at the lower mass region during the conversion process. The product ion, $Au_{135}(SCH_2CH_2Ph)_{57}^+$ has much larger width than $Au_{25}(SCH_2CH_2Ph)_{18}^+$ due to distribution in ligand composition as well as reduced resolution at higher mass range. Due to this reason, the exact composition of the product may have some variation. Nevertheless, only one product was seen.

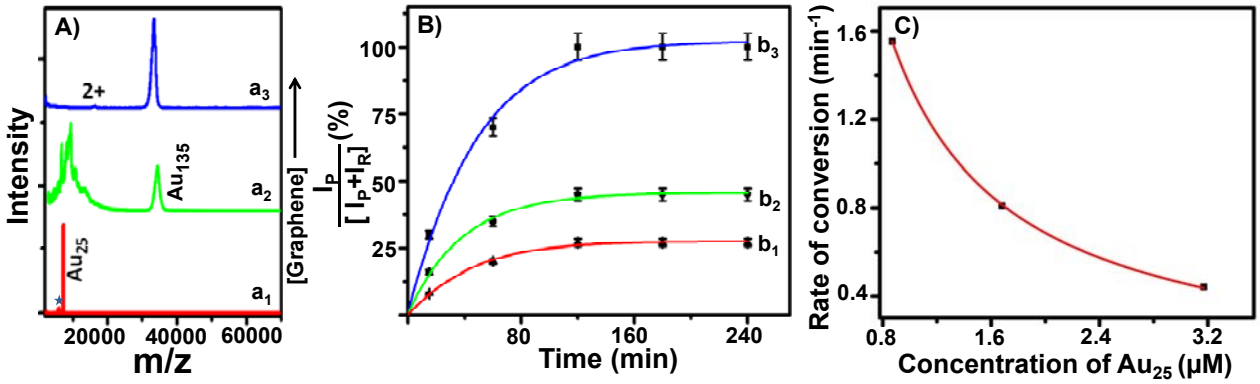


**Fig. 2.** A) MALDI MS spectra with increasing graphene concentration for a constant $Au_{25}$ concentration. $a_1$) Data corresponding to $Au_{25}$ alone. The peak marked * is due to a fragment. $a_2$) Data at lower concentration (0.005 wt %) of graphene where complete conversion of $Au_{25}$ to $Au_{135}$ has not taken place. It shows some peaks at lower mass. $a_3$) At higher concentration (0.01 wt %) of graphene, complete conversion to $Au_{135}$ has happened. Dication of $Au_{135}$ is marked on the above figure. B) Time dependent conversion of $Au_{25}$ for a fixed graphene concentration at different $Au_{25}$ concentrations. $I_P$ and $I_R$ represent the intensity of $Au_{135}$ and $Au_{25}$ in the MALDI MS spectra. Traces $b_1$, $b_2$, and $b_3$ represent concentrations of $Au_{25}$ (3.17, 1.68 and 0.87 μM respectively). Statistics refer to data from multiple measurements. C) A plot of slope vs. surface concentration derived from figure B.

The transformation is sensitive to both concentration of the cluster and graphene. For a given cluster concentration, increasing graphene content converts all the clusters to $Au_{135}$. As shown in Fig. 2A, at a lower

graphene concentration (0.005 wt %, trace $a_2$), $Au_{25}$ is observed even after 48 hours of reaction. At higher concentration (0.01 wt %, trace $a_3$) of graphene, conversion to $Au_{135}$ takes place where the $Au_{25}$ peak is not any more visible. Further, upon increasing cluster concentration, for a fixed graphene concentration (0.01 wt%), we see reduced conversion (Fig. 2B). While at lower cluster concentration all the clusters convert to $Au_{135}$, at increasing cluster concentration, more clusters remain without conversion. This reduced efficiency of conversion continued even upon a longer reaction time.

While the transformed clusters are less susceptible for electron beam-induced aggregation, the parent $Au_{25}$ is extremely sensitive to electron beam-induced aggregation and undergoes rapid coalescence. Smaller clusters such as $Au_{25}$ grow in size with exposure to electron beam.[27] The molecular nature of $Au_{135}$ is evident in the mass spectrum which exhibits a well-defined peak assigned to a specific composition. From the MALDI MS study, we have seen that $Au_{135}$ is resistant towards fragmentation upon increasing laser intensity used to perform desorption-ionization. Generally, clusters show severe laser intensity-dependent fragmentation in which more of lower mass ions are observed at increasing laser fluence. The increased stability observed is due to the fact that the clusters are attached to the graphene surface which efficiently removes the excitation energy.

The slope of the curves in Fig. 2 (B) gives the rate of conversion to $Au_{135}$ at different times. The rate is rapid at initial times and then slows down and finally becomes zero at very large times. The low time values of the rate of conversion, $k$ has been plotted as a function of the $Au_{25}$ surface concentration, $c$ on the graphene surface (Fig. 2C). The best fitted line shows that $k = \lambda/c$, the dynamical information being incorporated in λ which has the dimension $[L^2T]^{-1}$. Such dynamical quantity is dimensionally consistent with mean squared displacement (MSD) $\langle r^2 \rangle \propto t^{-1}$ over the surface as a function of time, $t$. Such MSD can be found if the particle motion is in a trapping potential of strength $V_0$ in the presence of strong damping Γ. The mean squared fluctuations from the trapping centre would decay as $\left[1 + \left(\frac{V_0}{\Gamma}\right)t\right]^{-1}$. Clearly the formation of $Au_{135}$ clusters from the parent $Au_{25}$ clusters is governed by the trapping of the smaller clusters in a deep potential well generated by the graphene surface.

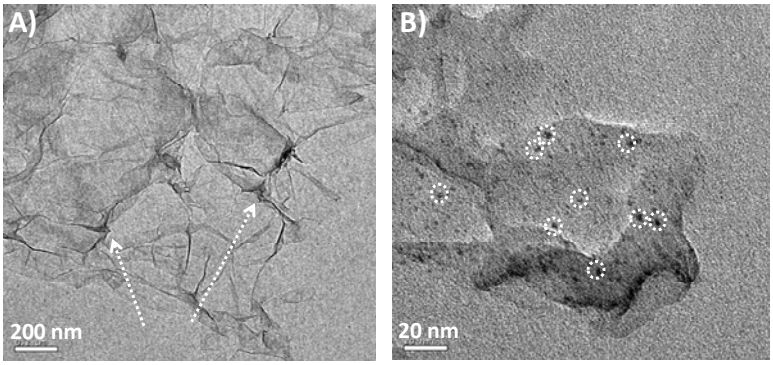


***Fig. 3.*** A) TEM image of chemically synthesized graphene alone. The nanometer thin folding (marked) indicates that the sheets imaged contain two-three layers of chemically synthesized graphene. B) Image of graphene surface containing clusters ($Au_{135}$). Some clusters are marked with circles. Outside the graphene surface, there was no cluster. It proves that the conversion happened only on graphene surfaces. Number of folding has decreased significantly in B.

Fig. 3 compares the TEM Images of chemically stable graphene and gold cluster-nucleated graphene. The size of $Au_{135}$ is in the 2 nm range which agrees with the observed particle sizes, which are the expected sizes of clusters of this range.[26] Number of folds of the sheets has reduced after the reaction (Fig. 3B). As the clusters are strongly adherent to the graphene surface, our efforts to separate $Au_{135}$ in solution for additional examination was unsuccessful.

The energy gain due to the reduction of the surface curvature may be the main drive to trap the smaller clusters, leading to their coalescence, as suggested by the concentration dependence of the conversion rate. Let us assume that the small clusters are driven by the curvature. The smaller clusters thus experience chemical potential proportional to the local curvature on the surface. Let $h(\vec{r})$ be the height of the surface and $\rho(\vec{r})$ be the density of the smaller clusters on the surface at a point $\vec{r}$. The chemical potential experienced by the smaller clusters is then $\mu(\vec{r}) = \lambda\nabla^2 h(\vec{r})$, $\lambda$ being the coupling parameter. We use the density functional free energy for a strongly interacting classical system,[28] consisting of the smaller clusters and the surface. The Gibbs free energy of the system consists of several components: The entropy of the smaller clusters given by $\int d\vec{r}\rho(\vec{r})\ln(\vec{r})$; the entropy of height fluctuations of the surface $\int d\vec{r}h(\vec{r})\ln\ h(\vec{r})$; the contributions due to correlated changes in density of the smaller clusters and in the surface height, given by $-\left(\frac{1}{2}\right)\int d\vec{q}c(\vec{q})\delta\rho(\vec{q})^2$ and $-\left(\frac{1}{2}\right)\int d\vec{q}\alpha(\vec{q})\delta h(\vec{q})^2$, respectively. The wave vector modes $\delta\rho(\vec{q})$ and $\delta h(\vec{q})$ indicate heterogeneity with respect to the mean density and average surface height, while $c(\vec{q})$ and $\alpha(\vec{q})$ denote their correlations, respectively. Finally we add the contributions due to the chemical potential coupling between the smaller clusters and the surface, resulting in $\int \mu(\vec{r})\delta\rho(\vec{r})d\vec{r}$. The net free energy $F$ of the system is given by the sum of these contributions. The equilibrium heterogeneity of the structure spontaneously supported by the system is given by the simultaneous conditions $\frac{\partial F}{\partial\rho(\vec{q})} = \frac{\partial F}{\partial h(\vec{q})} = 0$. We consider the standard Ornstein-Zernike form for the correlation functions[28]: $c(q) = c_0/(q^2 + \xi_0^2)$, $\xi_0$ being the particle correlation length and $c_0$ related to the inverse of the bulk compressibility; and similarly $\alpha(\vec{q}) = \alpha_0/(q^2 + \xi_s^2)$, , $\xi_s$ being the correlation length of the surface height fluctuations and $\alpha_0$ given by the inverse of surface compressibility. For large $\lambda$, $L \approx q^{-1} \propto \lambda\xi_0/c_0^{1/2}$, for a given concentration of graphene. At very low particle densities, $c \approx 1$, the correlation length typically extends to a few particle diameters so that $L$ is about a few nanometers so far as $\lambda$ is a finite number. $L$ compares well to the size of $Au_{135}$ clusters. The theory of interacting fluids shows[28] that $c_0 \approx -\infty$ for a high density incompressible fluid and $c_0$ decreases with decreasing particle density. Thus lower density of the particles facilitates the formation of bigger clusters which is qualitatively supported by the experimental observations. On the other hand, $\lambda$ can be taken to increase with increasing graphene concentration so that the stabilization of large clusters would be favored, as found in the experiments.

In summary, we established the coalescence of clusters of finite size to form larger cluster at graphenic interfaces. In particular, the role of the interface has been ascertained by both experiments and model theoretical calculations in stabilizing the large clusters. Our methodology with diverse clusters and high surface area substrates will allow the creation of atomically precise clusters directly on such supports. Such materials are expected to be useful as novel catalysts. Extension of this study to fullerene and carbon nanotubes is expected to produce new clusters.

## Acknowledgement:

We thank the Department of Science and Technology, Government of India for constantly supporting our research program on nanomaterials. A.G. thanks the Council of Scientific and Industrial Research (CSIR) for a fellowship.

## Reference:

[1] W. D. Luedtke and U. Landman, Phy. Rev. Lett. **82**, 3838 (1999).

[2] L. Bardotti, P. Jensen, A. Hoareau, M. Treilleux, and B. Cabaud, Phy. Rev. Lett. **74**, 4694 (1995).

[3] B. Yoon, W. D. Luedtke, J. Gao, and U. Landman, J. Phys. Chem. B **107**, 5882 (2003)

[4] O. Cretu, A. V. Krasheninnikov, J. A. Rodrı´guez-Manzo, L. Sun, R. M. Nieminen, and F. Banhart, Phy. Rev. Lett. **105**, 196102 (2010).

[5] C. Wang, J. Li, C. Amatore, Y. Chen, H. Jiang, and Xue-Mei Wang, Angew. Chem. Int. Ed. **50**, 11644 (2011).

[6] P. K. Sahoo, B. Panigrahy, D. Li, and D. Bahadur, J. Appl. Phys. **113**, 17B525 (2013)

[7] L. Lu , J. Liu , Y. Hu , Y. Zhang , and W. Chen, Adv. Mater. **25**, 1270 (2013)

[8] A. M. Zaniewski, M. Schriver, J. G. Lee, M. F. Crommie, and A. Zettl, Appl. Phys. Lett. **102**, 023108 (2013)

[9] T.S. Sreeprasad, Shihabudheen M. Maliyekkal, K.P. Lisha, and T. Pradeep, J. Hazard. Mater. **186,** 921 ((2011)

[10] B. Wang, B. Yoon, M. Ko□nig, Y. Fukamori, F. Esch, U. Heiz, and U. Landman, Nano Lett. **12**, 5907 (2012)

[11] M. W. Heaven, A. Dass, P. S. White, K. M. Holt, and R. W. Murray, J. Am. Chem. Soc. **130**, 3754 (2008).

[12] M. Zhu, C. M. Aikens, F. J. Hollander, G. C. Schatz, and R. Jin, J. Am. Chem. Soc. **130**, 5883 (2008).

[13] C. Zeng *et al.,* Angew. Chem., Int. Ed. **51**, 13114 (2012)

[14] H. Qian, W. T. Eckenhoff, Y. Zhu, T. Pintauer, and R. Jin, J. Am. Chem. Soc. **132**, 8281 (2010).

[15] P. D. Jadzinsky, G. Calero, C. J. Ackerson, D. A. Bushnell, and R. D. Kornberg, Science **318**, 433 (2007).

[16] L. D. Menard, S.-P. Gao, H. Xu, R. D. Twesten, A. S. Harper, Y. Song, G. Wang, A. D. Douglas, J. Yang, A. I. Frenkel, et al. J. Phys. Chem. B **110**, 12874 (2006)

[17] G. Schmid, Chem. Soc. Rev. **37**, 1909 (2008).

[18] O. Lopez-Acevedo, J. Akola, R. L. Whetten, H. Grönbeck, and H. Häkkinen, J. Phys. Chem. C **113**, 5035 (2009)

[19] P. R. Nimmala and A. Dass, J. Am. Chem. Soc. **133**, 9175 (2011).

[20] Y. Shichibu, Y. Negishi, H. Tsunoyama, M. Kanehara, T. Teranishi, and T. Tsukuda, Small **3**, 835 (2007).

[21] T. Udayabhaskararao, and T. Pradeep, Angew. Chem., Int. Ed. **49**, 3925 (2010)

[22] A. Ghosh, T. Udayabhaskararao, and T. Pradeep, J. Phys. Chem. Lett. **3**, 2002 (2012).

[23] M. Zhu, E. Lanni, N. Garg, M. E. Bier, and R. Jin, J. Am. Chem. Soc. **130**, 1138 (2008).

[24] D. R. Dreyer, S. Park, C. W. Bielawski, and R. S. Ruoff, Chem. Soc. Rev. **39**, 228 (2010).

[25] D. Li, M. B. Muller, S. Gilje, R. B. Kaner, and G. G. Wallace, Nat. Nanotechnol. **3**, 101 (2008).

[26] I. Chakraborty, A. Govindarajan, J. Erusappan, A. Ghosh, T. Pradeep, B. Yoon, R. L. Whetten and U. Landman, Nano Lett. **12,** 5861 (2012)

[27] P. Ramasamy, S. Guha, E. S. Shibu, T. S. Sreeprasad, S. Bag, A. Banerjee, and T. Pradeep, J. Mater. Chem. **19,** 8456 (2009).

[28] J. –P. Hansen and I. R. McDonald, Theory of Simple Liquids (Academic, London, 1986).